Critical equation of seedling block falling off in transplanting process and the optimization experiment of rape blanket seedling transplanter

Lan Jiang, Chongyou Wu*, Qing Tang, Min Zhang, Gang Wang, Jun Wu

(*Nanjing Research Institute for Agricultural Mechanization, Ministry of Agriculture and Rural Affairs, Nanjing 210014, China*)

Abstract: Considering both high efficiency and high seedling standing quality is a significant objective for crop mechanized transplanting. Rape blanket seedling transplanting is an innovative and efficient transplanting technique. However, falling off phenomenon has become a common problem facing rape blanket seedling transplanting fields that causes seedling standing quality decrease and restricts crop growth. In this study, the rape blanket seedling of Ningza-1838 varieties and 35 d of seedling age was taken as the research object. The critical falling off equations of seedling was established by dynamic analysis. Main factors affecting seedling falling off were obtained. The critical value of each factor was calculated which were as follows: the rotation speed of the planting mechanism was 24.6 rad/s, the substrate moisture content was 50.4% and the longitudinal picking seedling quantity was 14.7 mm. Taking the seedling falling off rate as evaluation index, the measured critical value of seedling falling off was determined by high speed photography experiment. Under the condition that substrate moisture content was 55% and the longitudinal seedling quantity was 15 mm, the seedling falling off rate sharply increased when the transplanting mechanism rotation speed was increased from 24 rad/s to 26 rad/s. Under the condition that the rotation speed was 22 rad/s and the longitudinal picking seedling quantity was 15 mm, the seedling falling off rate rapidly decreased when the moisture content was increased from 47% to 53%. When moisture content exceeded 53%, this exhibited no obvious change. Under the condition that the moisture content was 50% and the rotation speed was 22 rad/s, the seedling falling off rate swiftly raised when the longitudinal picking seedling quantity was increased from 14 mm to 17 mm. The experimental results showed that the seedling falling off rate increased significantly near the critical value. The experimental results showed that the seedling falling off rate changed significantly near the critical value. It proved that the model was correct. Response surface experiments with the Box-Behnken design were conducted to determine the optimal combination parameters, which were as follows: substrate moisture content was 56.24%, planting mechanism rotation speed was 22.04 rad/s, and longitudinal picking seedling quantity was 14.91 mm. At this time, the seedling falling off rate was 1.36%, which ensured that seedlings could be transplanted stably under the carrier of seedling needle. The verification test was conducted, and the working parameters were adjusted according to the optimization results in experiment. The results of verification test were highly consistent with the optimization solution. The present study may provide a theoretical method for improving seedling standing quality of rape blanket seedling, and laid a foundation for the popularization and development of rape carpet seedling transplanting.

Keywords: rape blanket seedling, transplanter, planting mechanism, seedling falling off

DOI: 10.25165/j.ijabe.20191205.4537

Citation: Jiang L, Wu C Y, Tang Q, Zhang M, Wang G, Wu J. Critical equation of seedling block falling off in transplanting process and the optimization experiment of rape blanket seedling transplanter. Int J Agric & Biol Eng, 2019; 12(5): 87–96.

1 Introduction

Rape is an important oilcrop in China. The rice-rape and rice-rice-rape rotation cropping pattern are usually adopted[1-3]. In order to ensure the rape growth period, 30%-40% of the total area is planted through transplanting. Rape transplanting can shorten the growth period in native fields, which plays an important role in ensuring the stable and high yield of grain and rape[4-7]. At present, artificial transplanting is mainly used in rape transplanting in China, which has problems such as high labor intensity and high cost.

Mechanized transplanting equipment is mainly divided into manual transplanter, semi-automatic transplanter and full-automatic transplanter. The transplanting technology in developed countries is relatively mature, represented by large scale and fully automated. However, as a result of the planting system and mode, few foreign researches on rape transplanting technology have been reported. Major rape producing countries such as Germany, Australia, Canada, and France adopt mechanical direct-seeding. Research on rape transplanting technique in China started late, represented by semi-automatic. Fulai Agricultural equipment Co., Ltd develops 2ZQ-4 rape transplanter. The transplanting efficiency is about 40 plants/min by tests. Liu et al.[8] developed a drilling mechanism of rape transplanter for heavy soil conditions. Its transplanting efficiency is 50-60 times/min. The drilling mechanism has excellent drilling effect and the distance between holes can be kept even. Liao et al.[9] designed a conveyor belt type detaching device of transplanter for rape pot seedlings to solve

Received date: 2018-07-22 **Accepted date:** 2019-04-22

Biographies: Lan Jiang, Master, research interests: agricultural mechanization engineering. Email: jianglan0719@163.com; **Qing Tang**, Master, research interests: agricultural mechanization engineering. Email: 285881240@qq.com; **Min Zhang**, PhD, research interests: agricultural mechanization engineering. Email: zhm0912@126.com; **Gang Wang**, Master, research interests: agricultural mechanization engineering. Email: 421404047@qq.com; **Jun Wu**, Master, research interests: agricultural mechanization engineering. Email: 362268885@qq.com.

***Corresponding author**: **Chongyou Wu**, PhD, Professor, research interests: agricultural mechanization engineering. Nanjing Research Institute for Agricultural Mechanization, Ministry of Agriculture and Rural Affairs, Nanjing 210014, China. Tel: +86-15366092918, Email: cywu59@sina.com.

the problem of poor substrate integrality and poor transport stability during seedling separation. The current rape transplanting machine has a certain amount of technical characteristics, but there are still several defects, such as planting seedlings still rely on labor, and the whole process of mechanization cannot be realized. The rape transplanter has low efficiency, and cannot be adapted to paddy soil conditions[10-13].

In order to improve the present situation of rape transplanting, a rape blanket seedling transplanter was designed with the reference principle of the rice transplanter. The efficiency of the rape blanket seedling transplanter can reach up to 10 times higher than that of a traditional rape transplanter[14-17]. The high efficiency and seedling upright rate of a transplanter are the most crucial issues to achieve high quality transplantation. During the operation of the planting mechanism, the mechanism parameters and mechanical properties of rape blanket seedling can affect the integrality of seedling block and seedling-standing quality[18-22]. In the present study, it was found that the transplanting mechanism mainly used the adhesion and friction between the seedling needle, push rod and substrate of the rape blanket seedling, in order to complete the seedling transportation[18,23]. During the process of seedling transportation, seedling blocks occasionally fall off from the planting mechanism and into the soil, which seriously affects seedling upright quality. These problems have become a bottleneck in restricting the development of rape seedling transplanting mechanization. Research scholars have studied the mechanical characteristics of the pot seedlings and transplanting mechanism. Chen et al.[24] and Liu et al.[25] and Zhang et al.[26] studied the contact and collision movement of vegetable such as tomato and broccoli in the planting mechanism, so as to optimize the structural and performance parameters of the planting mechanism. Liu et al.[27] established the motion trajectory and angle variation equation of maize seedling in the process of transporting, and analyzed the seedling landing posture under different conditions. Nonetheless, the theoretical research on improving the transplanting quality of rape blanket seedling transplanter is still blank.

In the present, the dynamic model of rape blanket seedling block in the process of seedling transportation was established. The critical conditions for seedling falling off during the seedling transport process were investigated. The main factors that affected seedlings falling off and the critical value of each factor were obtained. The transplanting test for rape blanket seedlings was carried out using a single factor test and response surface test. The present study may provide a reference for the research and development of rape blanket seedling transplantation with high seedling upright quality.

2 Structure and working principle of a rape blanket seedling transplanter

2.1 Rape blanket seedling transplanter

The rape blanket seedling transplanter used in experiment is shown in Figure 1. It mainly consists of a furrow opener, seedling feeder mechanism, planting mechanism, compacting mechanism and chassis. The transplanter has a wide row spacing of 600 mm and a narrow row space of 300 mm. Furthermore, hole spacing was 120-200 mm, engine power was 12.8 kW, and transplant efficiency was 300-480 holes/row/min.

When the equipment operates, the transplanter engine provides motive power, which drives the spindle to rotate through the hydraulic system. Under the action of traction force and transplanter gravity, the corrugated disc furrow opener loosens the soil for ditching. Then, the rape seedling block is inserted into the seedling ditch, which is kept upright by relying on the soil and seedling ditch wall. Finally, the soil on both sides of the seedling ditch is squeezed around the seedling through the V-shaped compacting mechanism, and the seedling is compacted and consolidated.

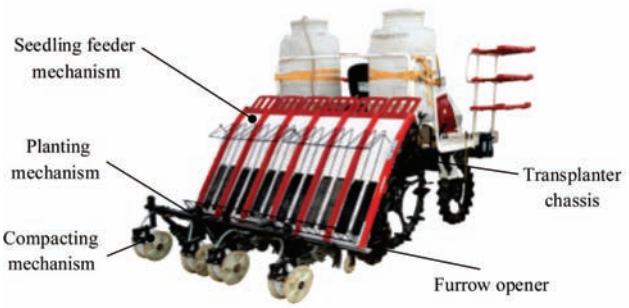

Figure 1 Rape blanket seedling transplanter

2.2 Planting mechanism

The planting mechanism of a rape blanket seedling transplanter is the transplanting mechanism with planetary elliptic gears, which comprises of the sun gear, middle gear, planet gear, planet carrier, planting arm, seedling pushing device and seedling needle (Figure 2). The sun gear is fixed to a frame, the planet carrier is a driving member, the planting arm is fixed to the planet carrier, the seedling needle is fixed in front of the planting arm, and the push rod of the seedling pushing device is installed on the inside of the seedling needle, which realizes the intermittent pushing of seedlings through cam rotation[28-30].

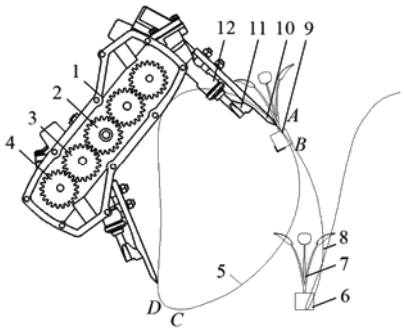

1. Planet carrier 2. Sun gear 3. Middle gear 4. Planet gear 5. Static trajectory 6. Substrate 7. Seeding 8. Dynamic trajectory 9. Picking seedling position 10. Seedling needle 11. Push rod 12. Planting arm

Figure 2 Structural diagram of the planting mechanism

When the planting mechanism operates, the planet carrier rotates clockwise and drives the planet gear to rotate at a non-constant-speed, in order to realize the reciprocating swing of the planting arm. The absolute motion of the needle tip on planting arm comprises of the uniform rotation around the planet carrier and the unequal speed rotation around the rotation center of the planet gear. Based on dryland soil properties, rape blanket seedling transplanting characteristics and the condition of vertical seedling, the planting trajectory with a large dip pushing angle and a vertical fast return was designed. The design parameters of the planting mechanism are presented in Table 1.

The planting process can be divided into four stages: picking seedling (*AB*), transporting seedling (*BC*), pushing seedling (*CD*), and returning (*DA*). During planting, the planet carrier rotates at high speed. Seedling needle tears the seedling block from the seedling tray by shear force, and moves the seedling block

according to the planting trajectory. When the needle reaches the pushing position, the spring of the seedling pushing device matches the cam rotation to push the push rod out. The seedling block is separated from the seedling needle, and planted into the soil. In order to avoid knocking down the transplanted seedling in the return course, the seedling needle returns quickly, and rotates to the position of the picking seedling for the next planting exercise.

Table 1 Major design parameters of the planting mechanism

Parameters	Values
Elliptic gear tooth number	21
Elliptic gear modulus	2
Elliptic gear eccentricity	0.152
Length of the seedling needle tip and planet gear center/mm	162
Initial installation angle of planet carrier/(°)	35
Initial installation angle of planting arm and planet carrier/(°)	58

2.3 Rape blanket seedling

In order to adapt the requirement of the transplanting machine, rape blanket seedlings are provided with characteristics of high density, small but strong seedlings, and strong packing root (Figure 3). After the preliminary experiments on the morphological characteristics and physical parameters of rape blanket seedlings and several years of field experiments, rape density was determined as 4000-5000 plants/m^2[18]. When the breeding procedure is finished, the well-developed lateral roots are bound with substrate, forming a seedling blanket that has strength and elasticity. After transplanting the seedling, the lower part is the substrate block, while the upper part was the seedling. The size of the single transplanted matrix was determined through the longitudinal picking seedling quantity and feed-time, which was defined as 12 times in a longitudinal picking seedling quantity through the test of picking seedling effect. The longitudinal picking seedling quantity can be adjusted in the range of 8-17 mm.

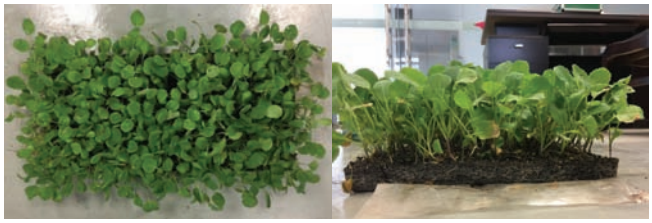

Figure 3 Rape blanket seedling

3 Dynamic analysis of the transplantation process

According to the transmission characteristics of the fixed axis gear train for the elliptical gear, a mathematical model of the planting mechanism was established. As shown in Figure 4, the rectangular coordinate system is established by taking the rotation center of the planet carrier of the transplanting mechanism with the planetary elliptic gears as the origin. Thus, the dynamic trajectory displacement equation of the seedling needle tip E is obtained, as follows:

$$\begin{cases} x_d = 4i\cos(\alpha_H - \varphi_H) + L\cos(\alpha_H - \alpha_0 - \varphi_3) + \varphi_H \cdot H / \pi \\ y_d = 4i\sin(\alpha_H - \varphi_H) + L\sin(\alpha_H - \alpha_0 - \varphi_3) \end{cases} \quad (1)$$

where, x_d is the dynamic trajectory of the seedling needle tip in the *X-axis*, mm; y_d is the dynamic trajectory of the seedling needle tip in the *Y-axis*, mm; H is plant spacing, mm; i is the long-axis radius of the pitch curve for the elliptic gear, mm; α_H is the installation angle between the planet carrier and *X-axis*, rad; φ_H is the planet carrier rotation angle, rad; α_0 is the installation angle between the planet carrier and planting arm, rad; φ_3 is the planet gear rotation angle, rad; and L is the length of the seedling needle tip and planet gear center, mm.

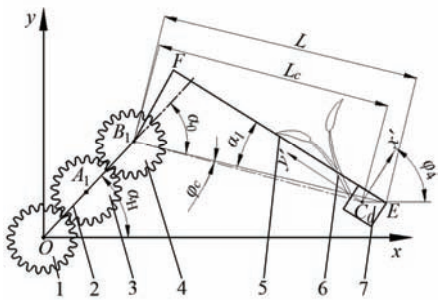

1. Sun gear 2. Planet carrier 3. Middle gear 4. Planet gear 5. Seedling needle 6. Rape seedling 7. Substrate

Figure 4 Kinematic diagram of the seedling transportation process

After seedling extraction, the substrate is inside the seedling needle. An angle between 15° and 25° is naturally formed due to the combination of the seedling and the outside of the seedling needle, which is defined as 20°. The dimension relationship between the mass center and seedling needle tip is established, as shown in Equation (2) and (3). The offset coordinate of the mass center relative to the seedling needle tip is defined as (x_c, y_c). The *3D* model of Ningza-1838 rape blanket seedling was established to determine the mass center position (C_0) of the seedling block.

$$L_c = \sqrt{(L\sin\alpha_1 - x_c)^2 + (L\cos\alpha_1 - y_c)^2} \quad (2)$$

$$\varphi_c = \arctan\left(\frac{L\sin\alpha_1 - x_c}{L\cos\alpha_1 - x_c}\right) \quad (3)$$

where, L_c is the distance between the mass center and planet gear rotation center, mm; φ_c is the angle of the connecting line between the needle tip and planet gear rotation center and the connecting line between the mass center and planet gear rotation center, rad; α_1 is the angle of the seedling needle and the connecting line between the needle tip and planet gear rotation center, rad; and α_1=0.13π was determined through the structural parameters of the planting arm.

The acceleration equation of the seedling needle tip E is obtained through the second derivation of Equation (1). Combined with Equation (2) and (3), and based on Newton's second law, the force relation of a seedling block moving according to the planting trajectory is calculated as:

$$\begin{cases} F_x = -4imw^2\cos(a_H - \varphi_H) - L_c mw^2\cos(a_H - a_0 - \varphi_c - \varphi_3)\cdot i_{3H}\cdot\dot{i}_{3H} \\ F_y = -4imw^2\sin(a_H - \varphi_H) - L_c mw^2\sin(a_H - a_0 - \varphi_c - \varphi_3)\cdot i_{3H}\cdot\dot{i}_{3H} \end{cases} \quad (4)$$

where, F_x is the resultant force of the seedling block mass center in the *X-axis* of the absolute coordinate system, N; F_y is the resultant force of the mass center of the seedling block in the *Y-axis* of the absolute coordinate system, N; i_{3H} is the transmission ratio of the planet gear relative to the planet carrier; w is the rotation angular velocity of the sun gear; and m is the mass of the picked seedling block.

In order to expediently calculate, the dynamic coordinate system, which takes the seedling block mass center as the origin and the direction of the vertical seedling needle as the *X-axis*, is established, as is shown in Figure 4. Equation (5) is the force relation of the seedling block after transforming the coordinate system.

$$\begin{cases} F_x' = F_x\cos\varphi_4 + F_y\sin\varphi_4 \\ F_y' = -F_x\sin\varphi_4 + F_y\cos\varphi_4 \end{cases} \quad (5)$$

$$\varphi_4 = 2/\pi - (\alpha_0 - \alpha_H + \alpha_1 + \varphi_3) \quad (6)$$

where, F_x' is the resultant force of the mass center of the seedling block in the *X-axis* of the transformation dynamic coordinate system, N; F_y' is the resultant force of the mass center of the seedling block in the *Y-axis* of the transformation dynamic coordinate system, N; and φ_4 is the angle between the *X-axis* of the dynamic coordinate system and horizontal plane, rad.

The force relation curve of the seedling block is drawn using MATLAB. As shown in Figure 5, the resultant force is initially negative, and becomes positive in the *X-axis*, which decreases in the negative *X-axis* and increases in the positive axis. It is always positive in the *Y-axis*, which gradually increases. When the resultant force of the seedling block on the *X*-axis is in the same direction of the gravity on the *X-axis*, the numerical relationship between F_x' and G_x affects the relative movement tendency of the seedling block. Therefore, the force condition of the seedling block during the seedling transportation process is divided into three stages:

1) The force in the *X*-axis is negative, $F_x' \geq G_x$. The force in the *Y-axis* is positive. At this time, the resultant force is located in the II quadrant of the dynamic coordinate system;

2) The force in the *X*-axis is negative, $F_x' < G_x$. The force in the *Y-axis* is positive.

3) The *X*-axis force is positive. The *Y*-axis force is positive. At this time, the resultant force is located in I quadrant of the dynamic coordinate system.

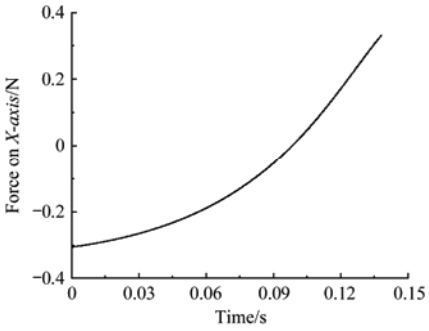

a. Resultant force of the seedling block mass center in the *X*-axis of the dynamic coordinate system

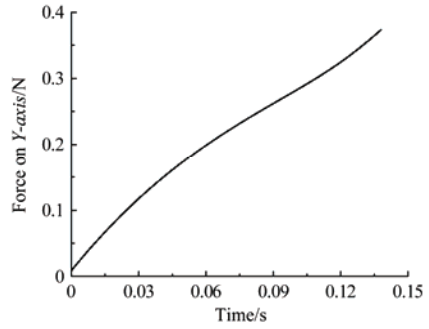

b. Resultant force of the seedling block mass center in the *Y*-axis of the dynamic coordinate system

Figure 5 Force relation curve of the seedling block in the seedling transport process

When the rape blanket seedling is removed from the feeding box, the upper surface of the substrate is attached to the push rod, and the side of the substrate is mainly attached to the inner wall of the seedling needle. Due to the tearing force in the picking process and substrate elastic deformation, the substrate size would be larger than the seedling needle. Thus, the partial substrate is attached to the upper surface of the outer wall of the seedling needle. During the seedling transportation process, the seedling block is subjected to gravity and contact forces. When these forces are not enough to provide the force required for the seedling block to motion according to the planting trajectory, the seedling block slips along the vertical direction of the seedling needle and drops out.

The force analysis on the seedling block in stage one is shown in Figure 6. The seedling block mass center is defined as the origin, and the direction of the vertical seedling needle is defined as the *X-axis*. The seedling falling off condition is obtained by analyzing the force of the seedling block on the planting mechanism.

$$\begin{cases} F_y' > F_{fs1} + \tau_s + \tau_c + P_d - G\cos\varphi_4 \\ F_x' = F_{ns1} + P_{s2} + G\sin\varphi_4 \\ F_{fs1} = F_{ns1}\cdot f \end{cases} \quad (F_{cx}' \geq G_x) \quad (7)$$

where, F_{fs1} is the friction of the substrate and the upper surface of the seedling needle inner wall, N; τ_c is the shear adhesion force of the substrate and the side of the seedling needle inner wall, N; τ_s is the shear adhesion force of the substrate and the upper surface of the seedling needle inner and outside walls, N; P_d is the normal adhesion force of the substrate and push rod, N; F_{ns1} is the normal supporting force of the substrate and the upper surface of the seedling needle inner wall, N; P_{s2} is the normal adhesion force of the substrate and the upper surface of the seedling needle outside wall, N; and f is the friction coefficient.

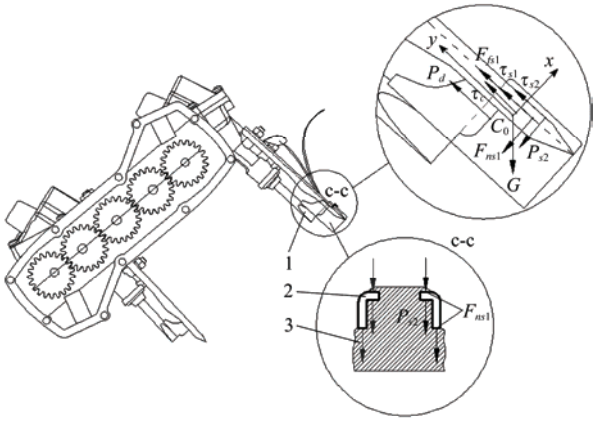

Figure 6 Force analysis on the seedling block in stage one

As shown in Figure 7a, the seedling falling off condition during stage two could be obtained, as follows:

$$\begin{cases} F_y' > \tau_s + \tau_c + P_d - G\cos\varphi_4 \\ F_x' = G\sin\varphi_4 - P_{s1} \end{cases} \quad (F_{cx}' < G_x) \quad (8)$$

where, P_{s1} is the normal adhesion force of the substrate and the upper surface of the seedling needle inner wall, N.

As shown in Figure 7b, the seedling falling off condition during stage three could be obtained, as follows:

$$\begin{cases} F_y' > \tau_s + \tau_c + P_d + F_{fs2} - G\cos\varphi_4 \\ F_x' = P_{s1} + F_{ns2} - G\sin\varphi_4 \\ F_{fs2} = F_{ns2}\cdot f \end{cases} \quad (9)$$

where, F_{fs2} is the friction of the substrate and the upper surface of the seedling needle outside wall, N; F_{ns2} is the normal supporting force of the substrate and the upper surface of the seedling needle outside wall, N.

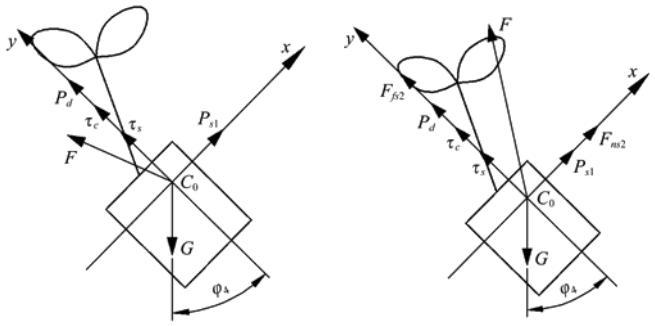

a. Force analysis on the seedling block in stage two b. Force analysis on the seedling block in stage three

Figure 7 A schematic diagram of the force on the seedling block

4 Application and test for the condition equation of seedling falling off

4.1 Morphological characteristics of rape blanket seedling

The morphological characteristic parameters of the rape blanket seedlings required in above dynamic model were obtained by experiment. The variety of rape applied in the test was Ningza-1838 and the seedling age was 35 d. A 280 mm×580 mm tray was used to cultivate the seedlings. The rape blanket was sliced with a cutter and sampled, and each of which had complete substrates and single seedlings, as shown in Figure 8. Thirty samples were randomly selected for measuring dimensions using a vernier calliper (MNT-200, Shanghai Meinaite Metals Instruments Co., Ltd, China) with a sensitivity of 0.02 mm. A digital counting balance (JM Industry co., Ltd, China) with an accuracy of 0.01 g was employed for measuring the mass of seedling and substrate. The results are shown in Table 2.

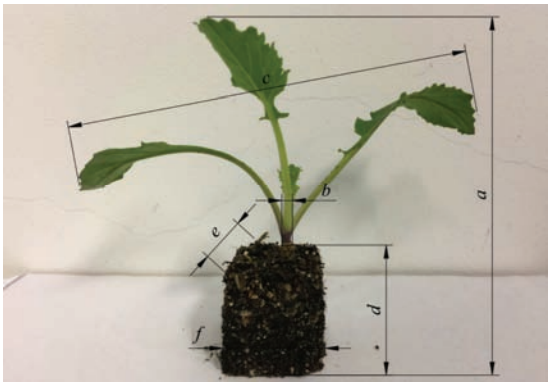

Figure 8 Force analysis on the seedling block in stage one

Table 2 Characteristic parameters of rape blanket seedlings

Parameters	Range	Mean	Variation coefficient/%
Seedling height/mm	115.62-126.12	119.38	11.79
Rhizome diameter/mm	1.72-2.14	1.84	16.39
Seedling width/mm	68.34-80.02	74.91	22.15
Seedling mass (without root)/g	0.65-0.88	0.73	12.84
Substrate density/kg·m^{-3}	810-990	880	10.60
Substrate thickness/mm	18.76-21.48	20.03	4.25
Picked substrate dimension (length×width)/mm	—	23.33×(8-17)	—

4.2 Physical characteristic parameter experiment of substrate

When the substrate part had contact with the planting mechanism, adhesion and friction occurred. Based on the theory of adhesion and friction of soil to metal materials, the unit normal adhesion force of soil is defined as[30]:

$$T=\frac{P}{S} \tag{10}$$

where, T is the unit normal adhesion force, N/cm^2; P is the tension required to separate from the adhesive surface, which acts on the vertical direction of the projectile interface, N; and S is the contact projection area between soil and non-soil objects in the vertical direction, cm^2.

The friction resistance of soil consists of shear adhesion force and friction[30].

$$F_\tau=\tau+F_n f \tag{11}$$

where, F_τ is the friction resistance, N; τ is the shear adhesion force, N; F_n is the normal load, N; f is the friction coefficient.

The substrate of rape blanket seedling was cut into 10 cm× 10 cm samples by a rectangular cutter, and its mass was measured by a digital balance. The seedling needle stuck into substrate to cut the seedling block, and contacted with the inner part of substrate during the process of seedling transporting. Therefore, the roots at the base of substrate were cut off to expose the inner part of substrate. The normal adhesion force was measured by universal testing machine (2450-200, INSTRON, America). A stainless steel plate made of the same material as the seedling needle is placed under the tester and a V-type clamp is installed A stainless steel plate made of the same material as the seedling needle was placed under the tester and a V-type fixture was installed. The sample was placed on the stainless steel plate, the center of which was aligned with the center of V-type fixture. The seedlings at the center of the substrate were tied together with a soft rope. Fixture took the rope and pulls it up until the sample was completely separated from the steel plate. The tensile rate of the tester was set to 1 mm/s. The maximum tensile force obtained by test minus sample mass is normal adhesion force. In the test of measuring shear adhesion force and friction coefficient, the substrate was cut into same size and placed horizontally on the stainless steel plate. The side of substrate was surrounded and fastened by a flat soft rope. The tension meter was connected to the ring port and is drawn slowly until the specimen moves. The maximum tensile force during the test is the friction resistance of the substrate. A tensionmeter (HP-30, Yueqing Handpi Instruments Co., Ltd, China) was used to connect with the soft rope and dragged slowly along the horizontal direction until the sample moved. The maximum tension recorded in test was the friction resistance of the substrate. Weights of different mass were placed on the substrate to change the normal pressure. The weights were selected as 150 g, 300 g, 450 g and 600 g. Based on Equation (13), the friction resistance under different weights was fitted linearly. The slope of fitting function was friction coefficient. The intercept from *Y-axis* was shear adhesion force.

The moisture content of substrate was set in the range of 44% to 64%. An infrared moisture determination balance (FD-720, Kett, Japan) was used to measure the moisture content of substrate with drying method. A five-point method was applied to sample the substrate in the same tray, and the average value of them was used as the moisture content of substrate in this tray. As shown in Figure 9, the relationship between the unit normal adhesion force, unit shear adhesion force, friction coefficient and moisture content was investigated by regression analysis, and all tallied with the parabolic distribution. Three fitted equations and correlation coefficients were expressed.

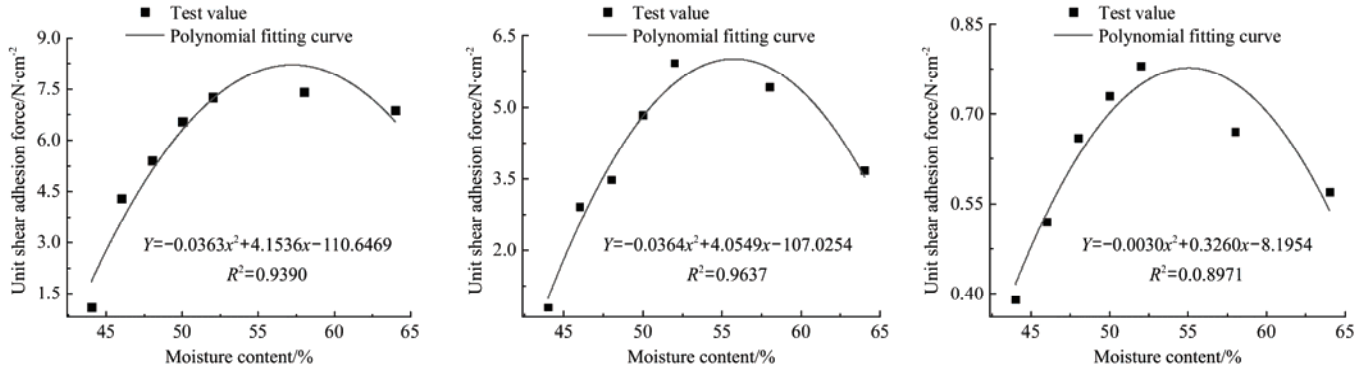

a. Regression curve of the unit normal adhesion force and substrate moisture content

b. Regression curve of the unit shear adhesion force and substrate moisture content

c. Regression curve of the friction coefficient and substrate moisture content

Figure 9 Regression curve of the physical characteristic parameter of the substrate

4.3 Motion analysis results of the seedling block

From the above theoretical analysis, it was found that the seedling falling off problem could be determined through the mass of the picked seedling block, substrate moisture content and rotation speed of the planting mechanism. Mass is adjusted through the longitudinal picking seedling quantity. By fixing two of these factors, the seedling falling off critical value of the other factor could be found.

When substrate moisture content was 55% and longitudinal picking seedling quantity was 15 mm, that seedling block mass was calculated to be 6.89 g combined with the test parameters in Table 2, the unit normal adhesion force (T_1) was calculated to be 0.0892 N/cm^2 using the fitting function in Table 2. Similarly, the unit shear adhesion force (C_1) was calculated to be 0.0710 N/cm^2, and the friction coefficient (f_1) was calculated to be 0.66. The seedling needle with a width of 20 mm and the matching push rod were selected for this test. The normal contact area between the substrate and the upper surface of seedling needle outside wall was measured as 0.36 cm^2. The normal contact area between the substrate and the upper surface of the seedling needle inner wall was 1.61 cm^2. The normal contact area between the substrate and the side surface of the seedling needle inner wall was 2.66 cm^2. The normal contact area between the substrate and push rod was 2.62 cm^2. The above data were substituted into the condition equation of seedling falling off in each stage, and the critical value of the transplanting mechanism rotation speed (w) was obtained as 24.6 rad/s. Similarly, when the rotation speed was 22 rad/s and the longitudinal picking seedling quantity was 15 mm, the substrate moisture content was calculated to be 50.4%. When the substrate moisture content was 50% and the rotation speed was 22 rad/s, the longitudinal picking seedling quantity was calculated to be 14.7 mm.

4.4 A study on the single factor test of the seedling block movement

(1) Materials and equipment

All tests were carried out in the test field of Nanjing Research Institute for Agricultural Mechanization, Nanjing, China. The condition of field test was shown in Figure 10. The Ningza-1838 rape cultivar was used in the experiments. The seedling age was 35 days. The equipment comprised of the experimental prototype of the rape blanket seedling transplanter, a high-speed camera (Redlake promotion X2), and a computer.

(2) Method

Based on the results of the seedling block motion analysis, the effects of the planting mechanism rotation speed, longitudinal picking seedling quantity and substrate moisture content on the performance of the seedling falling off rate were investigated. The moisture content was determined using the drying method.

Figure 10 Field experiment

The motion video of the planting process of the rape blanket seedling was recorded using a high speed camera. The shooting rate was determined as 200 frame/s[31,32]. A total of 50 planting processes were performed, which were guaranteed to have complete substrates, and the seedlings were randomly selected from the collected images in each group of experiments, which was recorded as N_0. The number of planting process samples that have fallen off the plant was recorded as N_1. The seedling falling off rate was defined as the assessment indicator, according to Equation (12).

$$\eta = \frac{N_1}{N_0} \times 100\% \quad (12)$$

where, η is seedling falling off rate, %; N_0 is the total number of planting processes for each group of test samples; and N_1 is the number of seedlings falling off.

(3) Results and analysis of the single factor test

Figure 11 was the experimental photograph taken with a high-speed camera. Based on the above theoretical analysis results and practical experience, the effect of the rotation speed of the planting mechanism within the range of 16-34 rad/s on the seedling falling off rate was investigated. The results are shown in Figure 12a. When the rotation speed of the planting mechanism was less than 24 rad/s, the seedling falling off rate was low, which remained unchanged. When the rotation speed was increased from 24 rad/s to 26 rad/s, this sharply increased. In the range of 24-32 rad/s, the seedling falling off rate increased with the increase in rotation speed. Therefore, a rotation speed of the planting mechanism at approximately 24 rad/s can be obtained as the critical range of seedling falling off. Figure 12b shows the effect results of the substrate moisture content in the range of 44%

to 65%. When the substrate moisture content was 44%-53%, the seedling falling off rate rapidly decreased with the increase in moisture content. When moisture content reached approximately 53%, this exhibited no obvious change. Therefore, the critical range of moisture content was approximately 53%. The effect of longitudinal picking seedling quantity in 9-17 mm on the seedling falling off rate is shown in Figure 12c. The seedling falling off rate initially decreases, and subsequently increases with the increase in longitudinal picking seedling quantity. This reached 14 mm when the seedling falling off rate reached a limited value of 10%. When the longitudinal picking seedling quantity reached 14-15 mm, the trend of the seedling falling off rate was balanced. As the longitudinal picking seedling quantity increasing above 15 mm, this rapidly increased. Combined with the images collected using the high speed camera, it was found that when the substrate moisture content was 50%, the quality of picking seedling exhibited a downward trend with the decrease in longitudinal picking seedling quantity. When the longitudinal picking seedling quantity was small, the substrate, which was irregular, dropped out in the seedling transporting process, thereby greatly increasing the seedling falling off rate. Thus, the longitudinal picking seedling quantity at approximately 14 mm could be obtained as the critical range of seedling falling off. The critical range of these three groups of single factor tests were close to the theoretical results. Consequently, the motion equation established in the present study was correct.

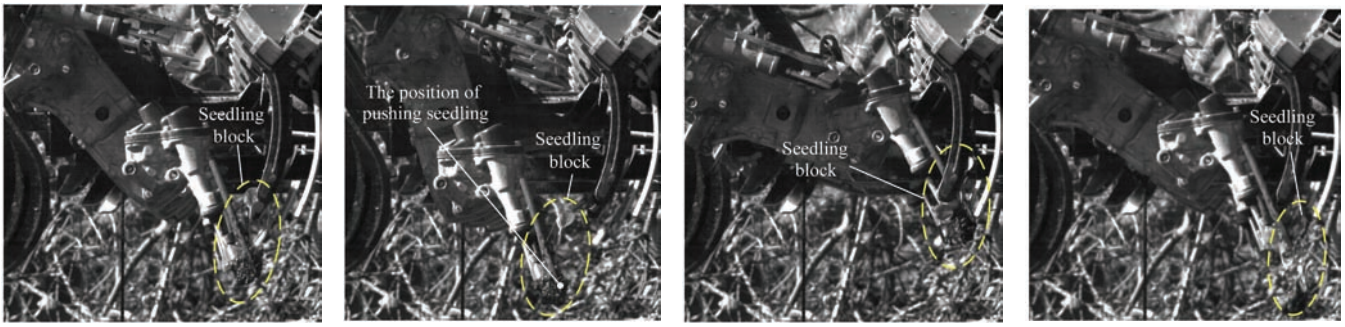

a. Transporting process without seedling falling off b. Pushing position without seedling falling off c. Transporting process before seedling falling off d. Seedling block separates form needle before reaching pushing position

Figure 11 Diagram of high-speed photography test performance

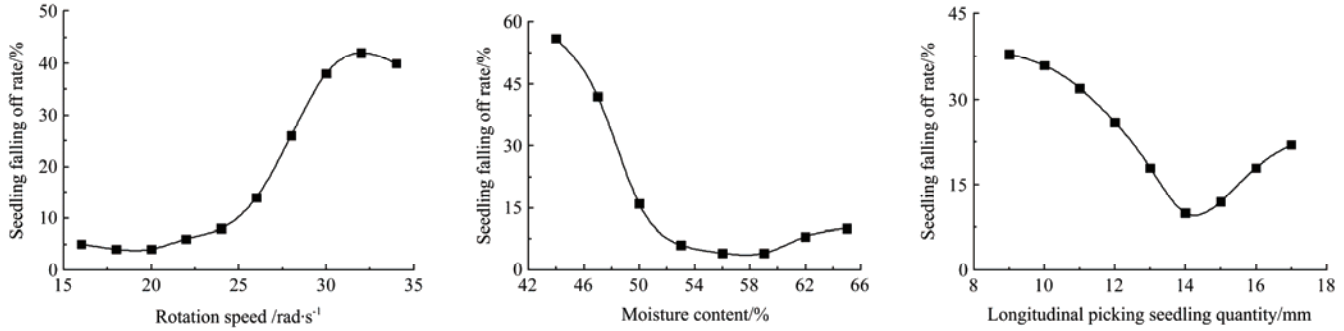

a. Seedling falling off rate with different planting mechanism rotation speeds b. Seedling falling off rate with different substrate moisture contents c. Seedling falling off rate with different longitudinal picking seedling quantities

Figure 12 Seedling falling off rate under different experimental factor

5 Parameter optimization of the planting process

The critical range of the planting mechanism rotation speed, vertical picking seedling quantity and substrate moisture content were determined using single factor tests. In order to obtain accurate optimization parameters, response surface experiments designed by Box-Behenken were conducted.

5.1 Experimental design

The value range selected for each factor was based on the results from the single factor experiments. A series of Box-Behenken design experiments was conducted to evaluate seedling falling off rate as a function of independent variables, namely, the planting mechanism rotation speed, longitudinal picking seedling quantity, and substrate moisture content. The factors and their levels are shown in Table 3. The measurement method of the performance index is the same as that of the single factor tests. A total of 17 group tests were conducted, and 200 planting processes were randomly selected in each group of experiments.

Table 3 Factors and levels of experiments

Levels	Substrate moisture content A/%	Planting mechanism rotation speed B/rad·s^{-1}	Longitudinal picking seedling quantity C/mm
–1	50	22	13
0	55	24	15
1	60	26	17

5.2 Test results and analysis

Based on the design and results of the Box-Behenken tests shown in Table 4, the Design Expert software was used to fit the regression models of the seedling falling off rate. The regression equations are listed in Table 5.

The p-value of the seedling falling off rate (Y) was less than 0.01. The regression model was extremely significant at a 95% confidence level. The p-value of lack of fit was greater than 0.05 (0.7040), indicating that the model had a high fitting degree. The coefficients of determination (R^2) exceeded 0.8, indicating that the model of the seedling falling off rate (Y) fitted the experimental results well.

Table 4 Experimental scheme and results

Serials number	Substrate moisture content *A*/%	Planting mechanism rotation speed *B*/rad·s^{-1}	Longitudinal picking seedling quantity *C*/mm	Seedling falling off rate *Y*/%
1	50	26	15	28
2	50	24	17	20.5
3	55	24	15	6
4	55	24	15	5
5	55	26	17	19
6	55	24	15	4
7	55	26	13	22
8	60	22	15	6
9	50	24	13	26.5
10	60	24	17	13.5
11	55	22	13	7
12	55	24	15	4
13	60	26	15	16
14	50	22	15	12.5
15	55	24	15	6.5
16	55	22	17	8
17	60	24	13	12.5

Table 5 Variance analysis of the regression equation

Source	Rate of seedling falling off			
	Sun of squares	Mean square	*F*-value	*P*-Value
Models	1009.42	112.16	110	<0.0001***
A	195.03	195.03	191.27	<0.0001***
B	331.53	331.53	325.14	<0.0001***
C	6.12	6.12	6.01	0.044*
AB	7.56	7.56	7.42	0.0296*
AC	12.25	12.25	12.01	0.0105*
BC	4	4	3.92	0.0881
A^2	229.79	229.79	225.36	<0.0001***
B^2	41.45	41.45	40.65	0.0004***
C^2	139.82	139.82	137.12	<0.0001***
Lack of fit	1.94	0.65	0.5	0.7040
Pure Error	5.2	1.30		
Total	1016.56			

Note: *** shows a significant difference (p<0.001), * shows a difference (p<0.05).

A multiple regression method was used to establish the regression equation for the influencing factors. For Equation (13), the effect of the primary items of *A* and *B* and the quadratic terms of A^2, B^2, and C^2 on the seedling falling off rate was extremely significant (p<0.001). The effect of the primary item *C* and the interaction terms *AB* and *AC* on the seedling falling off rate was statistically significant (p<0.05).

$$Y=5.10-4.94A+6.44B-0.88C-1.38AB+1.75AC-BC+7.39A^2+3.14B^2+5.76C^2 \quad (13)$$

The mutual interaction effects on the seedling falling off rate can be observed from the three-dimensional (3*D*) response surface plots in Figure 13. Figure 13a shows the effects of the longitudinal picking seedling quantity and the substrate moisture content on the rate of seedling falling off. When the longitudinal picking seedling quantity was 15 mm, the rate of seedling falling off initially decreased, and subsequently increased with the increase in substrate moisture content. Furthermore, the seedling falling off rate increased with the increase in rotation speed of the planting mechanism, and the rising rate was accelerated with the decrease in substrate moisture content. This was because the ability of soil consolidation with the seedling root significantly decreases when the moisture content of the substrate is low, and massive substrates are scattered and dropped in the process of seedling transportation when the rotation speed of the planting mechanism is high. As a result, plantlet instability occurs, and the seedling falling off rate is increased.

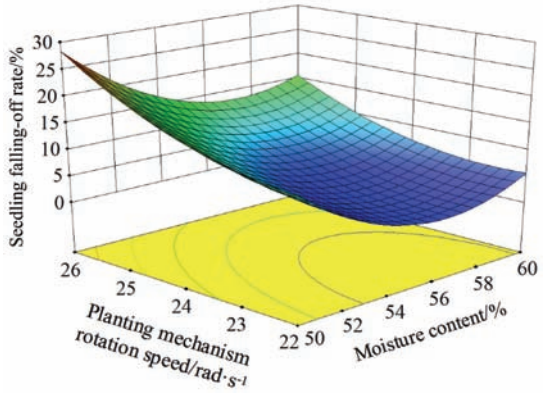

Note: The longitudinal picking seedling quantity is 15 mm.

a. Interaction effect between the planting mechanism rotation speed and substrate moisture content on the seedling falling off rate

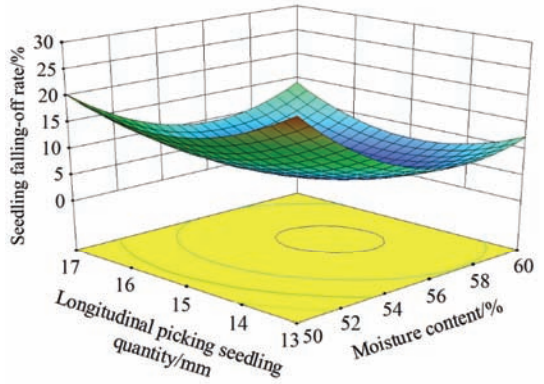

Note: The planting mechanism rotation speed is 24 rad/s.

c. Interaction effect between longitudinal picking seedling quantity and substrate moisture content on the seedling falling off rate

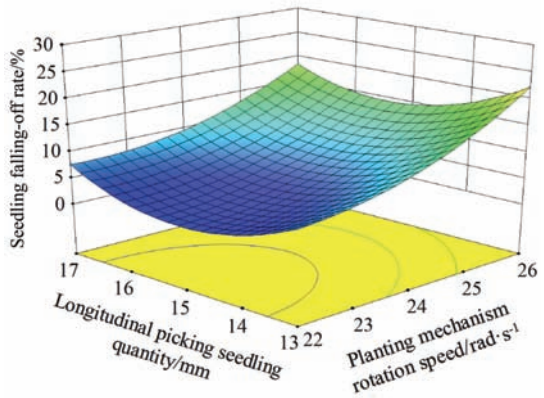

Note: The substrate moisture content is 55%.

c. Interaction effect between longitudinal picking seedling quantity and planting mechanism rotation speed on the seedling falling off rate

Figure 13 Interaction effects between factors on the seedling falling off rate

Figure 13b reveals the effects of the longitudinal picking seedling quantity and substrate moisture content on the rate of seedling falling off. When the planting mechanism rotation speed is 24 rad/s, the seedling falling off rate initially decreases, and subsequently increases with the increase in longitudinal picking

seedling quantity. Furthermore, with the decrease in substrate moisture content, the increase rate of the seedling falling off rate is accelerated. This was mainly because the reduction in longitudinal picking seedling quantity lead to the poor effect of picking seedlings, and the contact area of the incomplete substrate with the seedling needle and push rod was reduced during seedling transportation, resulting in a higher seedling falling off rate.

The effects of the longitudinal picking seedling quantity and planting mechanism rotation speed on the rate of seedling falling off are presented in Figure 13c. The seedling falling off rate initially decreases, and subsequently increases as the longitudinal picking seedling quantity increases, and decreases rapidly as the rotation speed increases. This is mainly because when the rotation speed of the planting mechanism is high, the impact action of the seedling needle on the seedling block is enhanced. Moreover, when the longitudinal picking seedling quantity is small, the capacity of the seedling block to resist the impact action of the seedling needle is weakened. Therefore, a better quality seedling block could not be obtained, resulting in a higher seedling falling off rate.

5.3 Optimization response and comparative test

The aim of the present study was to determine the optimal parameters required to achieve better characteristics of planting mechanism and rape blanket seedling. The optimization process was conducted using Design Expert software, assigning constraints 'in the range' for independent variables, and 'minimized' for the seedling falling off rate. The optimal conditions recommended by the software were a substrate moisture content of 56.24%, a planting mechanism rotation speed of 22.04 rad/s (adjusted to 22 rad/s), and a longitudinal picking seedling quantity of 14.91 mm (adjusted to 15 mm). Under optimal conditions, a seedling falling off rate of 1.36% was obtained. In order to verify the feasibility of the optimization results, the comparative test adopted the same method in the same place. The average value of the test was taken five times. Finally, the seedling falling off rate was obtained as 1.52%, and the relative error from the predicted value was 0.16%. The comparison of experimental and predicted results revealed that these were relatively similar, indicating that the models were highly reliable.

6 Conclusions

(1) In the working process of planting mechanism, rape blanket seedlings are transported under the control of seedling needle. In the middle of the transporting, when seedling blocks appear to be separated from the seedling needle and drop, the posture of seedling blocks are unstable extremely after falling on the soil, which produces serious dumping problems. Thus, a method to solve the problem of seedling falling off by establishing a dynamic model of seedling in the transporting process was proposed, which provided the foundation for improving the quality of rape blanket seedling transplanting.

(2) The parameters affecting contact force between seedling needle and rape blanket seedling substrate were as follows: normal adhesion force, shear adhesion force and friction coefficient. The physical characteristic experimental results showed that all of them had parabola distribution with the moisture content of substrate.

(3) The critical falling off equations of seedling was established. The main factors affecting seedling falling off were substrate moisture content, longitudinal picking seedling quantity and planting mechanism rotation speed. Under the control of two factors, the critical falling off value of the other factor was calculated by using the critical falling off equations. Taking seedling falling off rate as evaluation index, the single factor tests was carried out by high speed photography. The seedling falling off rate increased obviously near the critical value calculated by theoretical calculation. It was verified that the critical falling off equations were correct.

(4) The Box-Benhnken central composite experimental design principle was adopted with three levels and three factors. Under optimal conditions, the substrate moisture content was 56.24%, the planting mechanism rotation speed was 22.04 rad/s, and the longitudinal picking seedling quantity was 14.91 mm. A verification test was carried out with the above optimized parameters, and the seedling falling off rate was 1.52%. The relative error of the evaluation index and theoretical optimization value was only 0.16%.

Acknowledgements

The authors acknowledge that this research was financially supported by the National Natural Science Foundation of China (51575284), the National Key Research and Development Program of China (2017YFD0700804), and Funds for Modern Agricultural Industry Technology System Construction of China (CARS-13).

[References]

[1] Li X Y, Zuo Q S, Chang H B, Bai G P, Kuai J, Zhou G S. Higher density planting benefits mechanical harvesting of rapeseed in the Yangtze River Basin of China. Field Crops Research, 2018; 218: 97–105.

[2] Forleo M B, Palmieri N, Suardi A, Coaloa D. The eco-efficiency of rapeseed and sunflower cultivation in Italy. Joining environmental and economic assessment. Journal of Cleaner Production, 2018; 172: 3138–3153.

[3] Qiong H, Wei H, Yan Y, Xue K Z, Li J L, Jia Q S, et al. Rapeseed research and production in China. The Crop Journal, 2017; 5(2): 127–135.

[4] Fu D H, Jiang L Y, Annaliese S M, Xiao M L, Zhu L R, Li L Z, et al. Research progress and strategies for multifunctional rapeseed: A case study of China. Journal of Integrative Agriculture, 2016; 15(8): 1673–1684.

[5] Kusek G, Ozturk H H, Akdemir S. An assessment of energy use of different cultivation methods for sustainable rapeseed production. Journal of Cleaner Production, 2016; 112: 2772–2783.

[6] Li L H, Wang C, Zhang X Y, Sarker K K. Mechanized cultivation technology of seedling-growing bowl tray made of paddy-straw and its effects on rice production. International Agricultural Engineering Journal, 2015; 24(3): 97–103.

[7] Gu X B, Li Y N, Huang P, Du Y D, Fang H. Effects of planting patterns and nitrogen application rates on yield, water and nitrogen use efficiencies of winter oilseed rape (*Brassica napus* L.). Transactions of the CSAE, 2018; 34(10): 113–123. (in Chinese)

[8] Liu Z Y, Sun J, Chen C, Hu J K. A Design of the Drilling Mechanism for rape transplanter. Journal of Jiaxing University, 2017; 29(6): 89–93. (in Chinese)

[9] Liao Q X, Hu X P, Zhang Z, Liu M F. Analysis on detaching process of detaching device and seedling pot integrity about rape transplanter. Transactions of the CSAE, 2015; 31(16): 22–29. (in Chinese)

[10] Jin X, Li D Y, Ma H, Ji J T, Zhao K X, Pang J. Development of single row automatic transplanting device for potted vegetable seedlings. Int J Agric & Biol Eng, 2018; 11(3): 67–75.

[11] Satpathy S K, Garg I K. Effect of selected parameters on the performance of a semi-automatic vegetable transplanter. Ama Agricultural Mechanization in Asia Africa & Latin America, 2008; 39(2): 47–51.

[12] Wang Y W, He Z L, Wang J, Wu C Y, Yu G H, Tang Y H. Experiment on transplanting performance of automatic vegetable pot seedling transplanter for dry land. Transactions of the CSAE, 2018; 34(3): 19–25. (in Chinese)

[13] Kumar G V P, Raheman H. Automatic feeding mechanism of a vegetable transplanter. Int J Agric & Biol Eng, 2012; 5(2): 20–27.

[14] Guo L S, Zhang W J. Kinematic analysis of a rice transplanting mechanism with eccentric planetary gear trains. Mechanism & Machine

Theory, 2001; 36(11): 1175–1188.
[15] Ye B L, Yi W M, Yu G H, Gao Y, Zhao X. Optimization design and test of rice plug seedling transplanting mechanism of planetary gear train with incomplete eccentric circular gear and non-circular gears. Int J Agric & Biol Eng, 2017; 10(6): 43–55.
[16] Xin L, Lv Z J, Wang W Q, Zhou M L, Zhao Y. Optimal design and development of a double-crank potted rice seedling transplanting mechanism. Transactions of the ASABE, 2017; 60(1): 31–40.
[17] Ji J T, Jin X, Du X W, He Z T, Zhao Z H. Motion trajectory analysis and performance test of up-film punch transplanting mechanism. International Agricultural Engineering Journal, 2015; 24(2): 30–38.
[18] Wu C Y, Wu J, Zhang M, Tang Q. Research on machine transplanting techniques of blanket rapeseed. Journal of Chinese Agricultural Mechanization, 2016; 37(12): 6–10. (in Chinese)
[19] Wu J, Tang Q, Yuan W S, Wang S F, Wu C Y. Design and parameter optimization of ditching and compacting parts of rapeseed carpet seedling transplanter. Transactions of the CSAE, 2016; 32(21): 46–53. (in Chinese)
[20] Wang S F. Research on mechanism and parameter optimization of rapeseed mat seedling cutting and transplantation. MS dissertation. Beijing: Chinese Academy of Agricultural Sciences, 2016. (in Chinese)
[21] Jin X, Ji J T, Liu W X, He Y K, Du X W. Structural optimization of duckbilled transplanter based on dynamic model of pot seedling movement. Transactions of the CSAE, 2018; 34(9): 58–67. (in Chinese)
[22] Liu J D, Cao W B, Tian D Y, Ouyang Y N, Zhao H Z. Optimization experiment of transplanting actuator parameters based on mechanical property of seedling pot. Transactions of the CSAE, 2016; 32(16): 32–39. (in Chinese)
[23] Qian D H, Zhang J X. A summary of study of adhesion and friction between soil and metals. Transactions of the CSAM, 1984; 1: 69–78.
[24] Chen J N, Xia X D, Wang Y, Yan J J, Zhang P H. Motion differential equations of seedling in duckbilled planting nozzle and its application experiment. Transactions of the CSAE, 2015; 31(3): 31–39. (in Chinese)
[25] Liu J D, Cao W B, Tian D Y, Tang H Y, Zhao H Z. Kinematic analysis and experiment of planetary five-bar planting mechanism for zero-speed transplanting on mulch film. Int J Agric & Biol Eng, 2016; 9(4): 84–91.
[26] Zhang G F, Zhao Y, Chen J N. Characteristic analysis of rice plotted-seedling's motion in air and on turbination-type guide-canal. Journal of Zhejiang University (Engineering Science), 2009; 43(3): 529–534. (in Chinese)
[27] Liu H L, Zhang W. Study on trajectory path and landing form of corn planting seedling. Journal of Heilongjiang Bayi Agricultural University, 2016; 28(3): 124–128. (in Chinese)
[28] Kumar G V P, Raheman H. Development of a walk-behind type hand tractor powered vegetable transplanter for paper pot seedlings. Biosystems Engineering, 2011; 110(2): 189–197.
[29] Dai L, Sun L, Zhao X, Zhao Y. Parameters optimization of separating-planting mechanism in transplanter based on kinematics objective function. Transactions of the CSAE, 2014; 30(3): 35–42. (in Chinese)
[30] Jin X, Pang J, Ji J T, Du X W, He Z T, Wang S G. Experiment and simulation analysis on high-speed up-film transplanting mechanism. International Agricultural Engineering Journal, 2017; 26(3): 105-112.
[31] Li X Q, Ma L, Xiong S, Jin X, Geng L X, Ji J T. High-speed camera analysis of seed corn ear bare hand threshing. International Agricultural Engineering Journal, 2017; 26(1): 60-67.
[32] Wang J W, Tang H, Wang J F, Jiang D X, Li X. Measurement and analysis of restitution coefficient between maize seed and soil based on high-speed photography. Int J Agric & Biol Eng, 2017; 10(3): 102–114.